Computers & Geosciences 103 (2017) 92–98

Contents lists available at ScienceDirect

Computers & Geosciences

journal homepage: www.elsevier.com/locate/cageo

Research paper

Numerical simulation of electro-osmotic consolidation coupling non-linear variation of soil parameters

Hui Wu, Liming Hu*, Qingbo Wen

State Key Laboratory of Hydro-Science and Engineering, Department of Hydraulic Engineering, Tsinghua University, Beijing, 100084, PR China

ARTICLE INFO

Keywords:
Electro-osmotic consolidation
Numerical simulation
Excess pore water pressure
Degree of consolidation
Settlement

ABSTRACT

Electro-osmotic consolidation is an effective method for soft ground improvement. A main limitation of previous numerical models on this technique is the ignorance of the non-linear variation of soil parameters. In the present study, a multi-field numerical model is developed with the consideration of the non-linear variation of soil parameters during electro-osmotic consolidation process. The numerical simulations on an axisymmetric model indicated that the non-linear variation of soil parameters showed remarkable impact on the development of the excess pore water pressure and degree of consolidation. A field experiment with complex geometry, boundary conditions, electrode configuration and voltage application was further simulated with the developed numerical model. The comparison between field and numerical data indicated that the numerical model coupling of the non-linear variation of soil parameters gave more reasonable results. The developed numerical model is capable to analyze engineering cases with complex operating conditions.

1. Introduction

Electro-osmotic consolidation is an effective technique for the improvement of soft soil, which involves the movement of pore water in a soil-water system from the anode toward cathode under an external electrical field. Laboratory experiments and field applications have been conducted to investigate the dewatering and consolidation behavior of soil subjected to electro-osmosis, and these investigations have generated significant knowledge pertaining to this process (Bjerrum et al., 1967; Esrig and Gemeinhardt, 1967; Casagrande, 1983; Lockhart, 1983; Lo et al., 1991; Micic et al., 2001; Burnotte et al., 2004; Glendinning et al., 2007; Jeyakanthan et al., 2011; Hu et al., 2013; Wu and Hu, 2014; Wu et al., 2015a, 2015b, 2016). Based on the knowledge, theoretical models are developed to describe the behavior of soil upon electro-osmotic consolidation, and analytical solutions for pore water pressure and degree of consolidation are obtained. Esrig (1968) first proposed a one-dimensional (1D) theoretical model and derived the solution for the excess pore water pressure under different boundary conditions. Wan and Mitchell (1976) investigated the coupling effect of surcharge preloading and electro-osmotic consolidation. Following their pioneering work, two-dimensional (2D) and axisymmetric models were further developed and the corresponding analytical solutions were derived by assuming constant soil parameters and ignoring the stress-strain behavior (Shang, 1998; Su and Wang, 2003; Li et al., 2010; Xu et al., 2011; Wu and Hu, 2013b). The obtained analytical solutions from the above models can only be applied to problems with simple boundary conditions and geometries, and cannot account for the non-linear variation of soil parameters and the coupling effect of the multi-fields including pore-water movement, electrical current, stresses and displacements. Moreover, the complex geological conditions and irregular electrode configuration in field applications cannot be considered with the developed analytical methods.

Numerical approach has proved to be a useful method to predict the behavior of soil upon electro-osmotic consolidation with complex boundary conditions and geometries. Up to now, many numerical models have been proposed to simulate the dewatering and consolidation processes of the treated soil (Lewis and Humpheson, 1973; Rittirong and Shang, 2008; Hu et al., 2010, 2012; Wang et al., 2012; Zhou et al., 2013; Jeyakanthan and Gnanendran, 2013; Hu and Wu, 2014; Deng and Zhou, 2015; Yuan and Hicks, 2015). Lewis and Humpheson (1973) applied the finite element method to analyze the development of pore water pressure during electro-osmotic consolidation in a 2D model. Rittirong and Shang (2008) used the finite difference model to simulate the field test reported by Bjerrum et al. (1967). Jeyakanthan and Gnanendran (2013) developed a finite element formulation integrated with the elastoplastic modified cam clay model. Hu and Wu (2014) proposed a three-dimensional (3D) numerical model for electro-osmotic consolidation and analyzed the effect of electrode configuration and electrode depth. Yuan and Hicks

* Corresponding author.
E-mail addresses: hui-wu@mail.tsinghua.edu.cn (H. Wu), gehu@tsinghua.edu.cn (L. Hu), wenqb@mail.tsinghua.edu.cn (Q. Wen).

http://dx.doi.org/10.1016/j.cageo.2017.03.002
Received 14 April 2016; Received in revised form 25 February 2017; Accepted 1 March 2017
Available online 02 March 2017

(2015) came up with a numerical solution at large strains and verified the solution by comparing with the field test conducted by Burnotte et al. (2004). With these proposed numerical approaches, the development of pore water pressure and soil deformation can be analyzed. However, most of the previous numerical simulations ignore the non-linear variation of soil parameters during electro-osmotic consolidation. In fact, both the laboratory experiments and field tests have confirmed the change of soil parameters such as electro-osmosis conductivity, coefficient of volume compressibility and hydraulic conductivity during electro-osmotic consolidation (Burnotte et al., 2004; Jeyakanthan et al., 2011; Wu and Hu, 2013a). These changes, although being recognized, have been rarely considered in the numerical analysis.

In this paper, the effect of the stress-strain field and the non-linear variation of soil parameters was analyzed with a multi-field coupling numerical model for electro-osmotic consolidation, in which empirical formulas describing the non-linear variation of soil parameters were incorporated. Moreover, a field test reported by Burnotte et al. (2004) was back analyzed with the numerical model. The variation of electro-osmosis conductivity and coefficient of compressibility was summarized from the literature and incorporated in the numerical simulations. The complex boundary conditions and geometry, the irregular electrode configuration and the intermittence of current were also considered in the numerical simulations to investigate the capability of the numerical approach to solve practical problems with complex operating conditions.

2. Numerical model for electro-osmotic consolidation

The multi-field coupling numerical model for electro-osmotic consolidation in this study is developed from the theoretical model proposed by Hu and Wu (2014). The adopted assumptions include: 1) the soil is saturated and the soil skeleton is linear elastic; 2) the velocity of water flow due to electro-osmosis is directly proportional to the voltage gradient; 3) the water movement in soil is linear superposition of water flows due to electro-osmosis and hydraulic gradient; 4) the influence of electrophoresis, electrochemical reactions and streaming potential is neglected.

According to Hu and Wu (2014), the governing equation for water flow during electro-osmotic consolidation is derived from the continuity equation of pore water and can be expressed as,

$$\nabla\cdot(\mathbf{k}_{\mathrm{h}}\nabla H + \mathbf{k}_{\mathrm{e}}\nabla V) = -\frac{\partial \varepsilon_{\mathrm{v}}}{\partial t} = \frac{\partial}{\partial t}(\nabla\cdot\boldsymbol{u}) \tag{1}$$

in which $\mathbf{k}_{\mathrm{h}}$ and $\mathbf{k}_{\mathrm{e}}$ are hydraulic conductivity and electro-osmosis conductivity tensor, respectively; H and V are total water head and voltage; ε_{v} is the volumetric strain of soil mass; $\boldsymbol{u}$ is the vector of soil mass displacement.

The stress-strain behavior of soil is describes by Biot's theory as (Biot, 1941),

$$\nabla^2\boldsymbol{u} + \frac{1}{1-2\nu}\nabla(\nabla\cdot\boldsymbol{u}) - \gamma_{\mathrm{w}}\cdot\frac{2(1+\nu)}{E}\nabla(H-z) = 0 \tag{2}$$

in which ν is the Poisson's ratio; E is the Young's modulus; z is the elevation head; γ_{w} is the unit weight of water.

The governing equation for the electric field can be obtained from the law of conservation of electrical charge (Hu and Wu, 2014),

$$\boldsymbol{\sigma}_{\mathrm{e}}\nabla^2 V = C_{\mathrm{p}}\frac{\partial V}{\partial t} \tag{3}$$

in which $\boldsymbol{\sigma}_{\mathrm{e}}$ is the electrical conductivity tensor; C_{p} is the capacitance per unit volume.

The above Eqs. (1)–(3) together describe the coupled process for electro-osmotic consolidation. With the three equations, the finite element method is then employed to solve the practical problems for electro-osmotic consolidation according to the actual boundary and initial conditions.

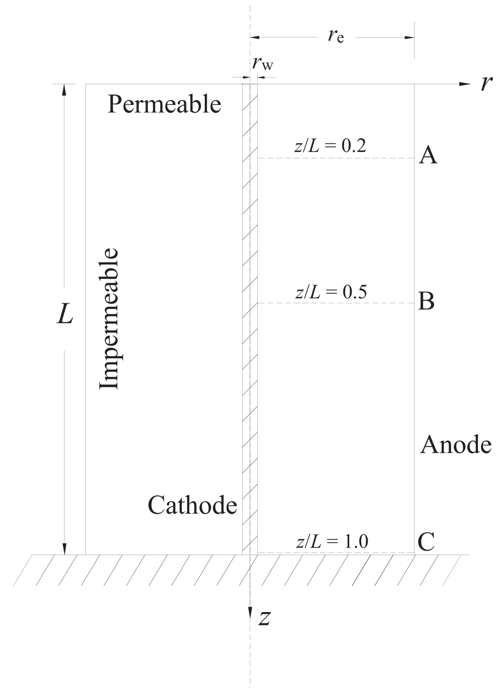

Fig. 1. Diagram of the axisymmetric model for electro-osmotic consolidation.

3. Effect of the stress-strain field and the non-linear variation of soil parameters

Wu and Hu (2013b) proposed an analytical solution for electro-osmotic consolidation under axisymmetric condition. However, the soil deformation was not considered during the mathematical derivation of the analytical solutions for pore water pressure and degree of consolidation. In order to analyze the coupling effect of stress-strain field on electro-osmosis, an axisymmetric model for electro-osmotic consolidation was developed as shown in Fig. 1. The top boundary and the cathode in the center were permeable, while the surrounding boundaries were impermeable. The adopted soil parameters and the size of the axisymmetric model were listed in Table 1. Two kinds of numerical simulations were performed on the axisymmetric model, including a numerical simulation that only considered the seepage and electrical fields and a fully coupling one. The results of the numerical simulations were further compared with that of the analytical solutions from Wu

Table 1
Soil parameters adopted in the numerical simulations and the size of the model.

Parameters	Values
Initial void ratio, e_0	2.0
Unit weight of water, γ_w (kN/m^3)	9.8
Saturated unit weight of soil, γ_s (kN/m^3)	20
Young′ modulus, E (kPa)	400
Poisson's ratio, ν	0.35
Initial effective stress, σ'_0 (kPa)	20
Compression index, C_c	0.20
Radial hydraulic conductivity, k_h (m/s)	5.0×10^{-9}
Vertical hydraulic conductivity, k_z (m/s)	2.5×10^{-9}
Radial electro-osmosis conductivity, k_e (m/s)	1.5×10^{-9}
Electrical conductivity, σ_e (S/m)	0.15
Capacitance per unit volume, C_p (Farad/m^3)	0
Applied voltage, V (V)	30
Radius of central cathode, r_w (m)	0.04
Radius of model, r_e (m)	0.5
Depth of model, L (m)	1

and Hu (2013b).

The relationships between soil parameters and void ratio, effective stress were obtained from previous studies (Archie, 1942; Mitchell and Soga, 2005; Rittirong and Shang, 2008; Hu et al., 2012; Wu et al., 2017),

$$
\begin{aligned}
k_h &= a\frac{e^3}{1+e}\ (\text{m/s}) \\
k_e &= b\frac{e}{1+e}\ (\text{m}^2/(\text{V s})) \\
m_v &= \frac{0.434C_c}{(1+e)\sigma'}\ (\text{MPa}^{-1}) \\
\sigma_e &= c\left(\frac{e}{1+e}\right)^m\ (\text{S/m})
\end{aligned}
\tag{4}
$$

in which k_h, k_e, m_v, and σ_e are hydraulic conductivity, electro-osmosis conductivity, coefficient of volume compressibility and electrical conductivity, respectively; e is the void ratio; C_c is the compression index; σ' is the vertical effective stress; a, b, c, and m are calculating factors for the four soil parameters. Generally speaking, with the change in void ratio, the change in k_h and m_v were more remarkable than that in k_e and σ_e. In order to analyze the effect of the non-linear variation of soil parameters, numerical simulations were performed with constant and variable soil parameters, respectively. The values of the initial void ratio e_0, initial effective stress σ'_0 and C_c were also displayed in Table 1. The values of the calculating factors a, b, c, and m were 1.875×10^{-9} m/s, 2.25×10^{-9} $\text{m}^2/(\text{V}\cdot\text{s})$, 0.467 S/m, and 2.8, respectively, and the initial values of the soil parameters (with an initial void ratio of 2.0) from the above empirical formulas were the same as that shown in Table 1.

Figs. 2 and 3 compared the excess pore water pressure and degree of consolidation obtained from the analytical solutions proposed by Wu and Hu (2013b), the numerical simulation without the coupling of stress-strain field, and the fully coupling numerical simulations with constant and variable soil parameters. The excess pore water pressure (absolute value) and degree of consolidation from the analytical solutions agreed well with those from the numerical simulation without the consideration of stress-strain field, and were larger than those from the fully coupling numerical simulation with constant soil parameters, especially in the early period of electro-osmotic consolidation. The non-linear variation of soil parameters showed remarkable impact on the development of the excess pore water pressure and degree of consolidation. As indicated by Eq. (4), k_h, k_e, m_v, and σ_e decreased with the

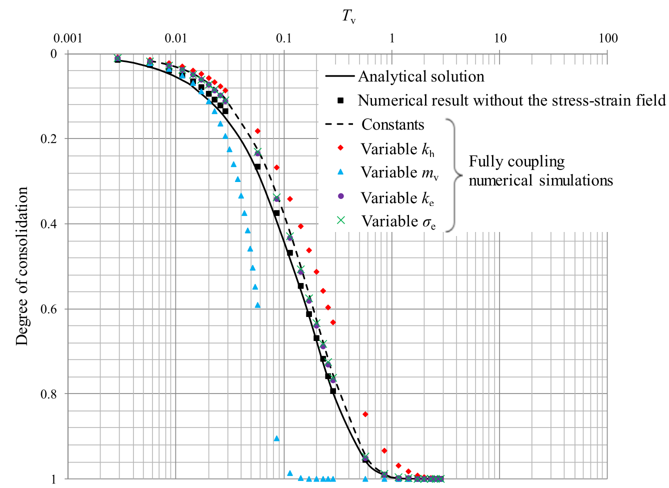

Fig. 3. Comparison of degree of consolidation from analytical solution and numerical simulations.

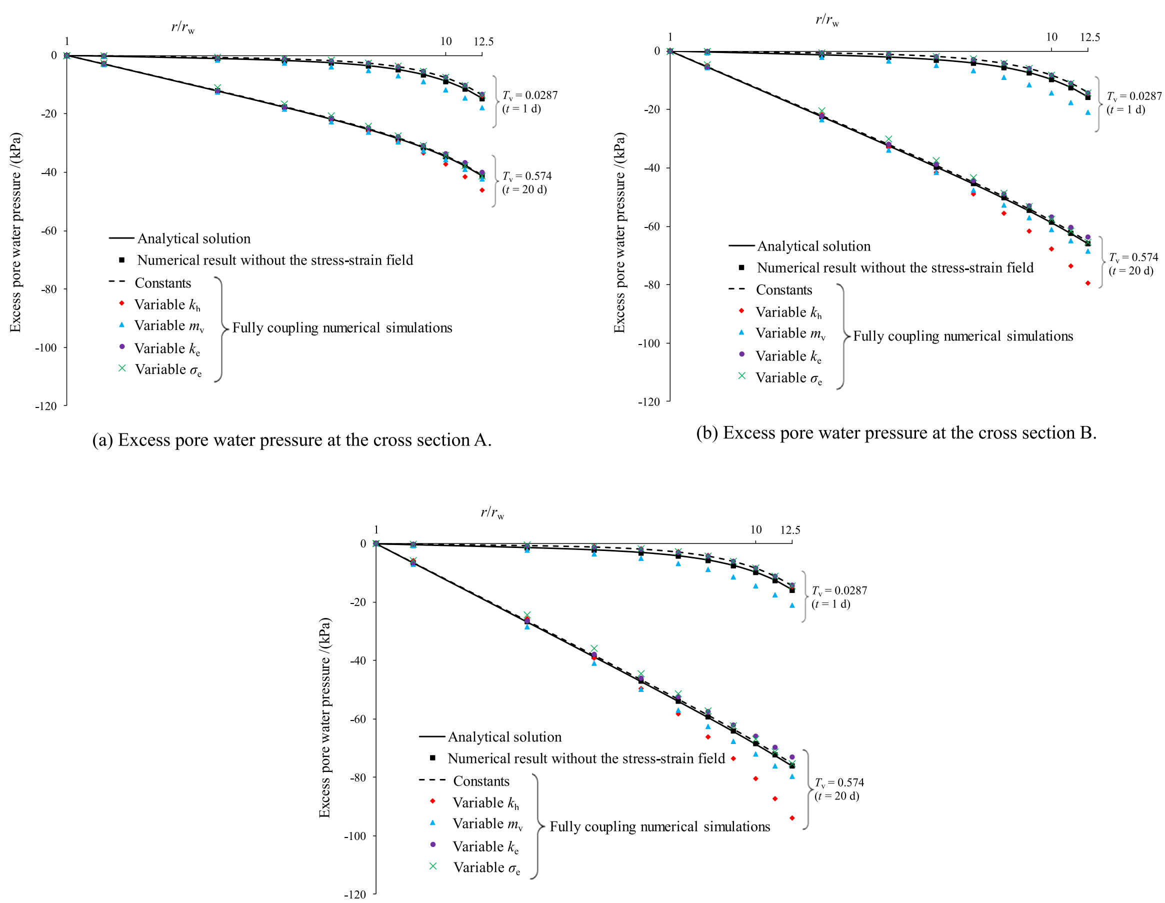

(a) Excess pore water pressure at the cross section A.

(b) Excess pore water pressure at the cross section B.

(c) Excess pore water pressure at the cross section C.

Fig. 2. Comparison of excess pore water pressure from analytical solution and numerical simulations at different positions.

decrease in void ratio and the increase in effective stress, which further affected the drainage and consolidation process. Compared to the numerical simulations with constant soil parameters, the numerical simulations with variable k_e and σ_e presented a slightly smaller excess pore water pressure (absolute value), while the numerical simulations with variable k_h and m_v presented a larger one. According to previous studies about electro-osmotic consolidation, the excess pore water pressure (absolute value) was positively related to k_e and negatively related to k_h, therefore the non-linear variation of k_h resulted in a larger excess pore water pressure (absolute value) while the non-linear variation of k_e caused a smaller one. The non-linear variation of m_v, on the other hand, led to the increase in the coefficient of consolidation, which then induced a larger excess pore water pressure (absolute value) at a specific time as shown in Fig. 2. Because the decrease in void ratio was generally larger near the anode, the decrease in σ_e was also larger near the anode. As a result, more voltage was applied on the soil near the anode and the voltage applied on the other parts of the soil decreased, which was detrimental to the electro-osmosis process and further caused the decrease in the excess pore water pressure (absolute value). Since the decreases in k_h and m_v were more significant than that in k_e and σ_e, the impacts of the non-linear variation of k_h and m_v were larger than that of k_e and σ_e. Moreover, the impact of the non-linear variation of k_h was more significant in the later period, while the impact of the non-linear variation of m_v was more significant in the early period.

The degree of consolidation was almost the same in the numerical simulations with constant parameters and that coupling the non-linear variation of k_e and σ_e. However, the non-linear variation of k_h resulted in a smaller degree of consolidation, and the non-linear variation of m_v caused a larger one. The degree of consolidation of soil treated by electro-osmotic consolidation mainly related to the coefficient of consolidation. Due to the decrease in k_h, the coefficient of consolidation decreased and the degree of consolidation was reduced; on the contrary, the decrease in m_v caused the increase in the coefficient of consolidation, and therefore the degree of consolidation increased.

The above analysis investigated the impacts of the non-linear variation of soil parameters on the excess pore water pressure and degree of consolidation. In fact, the impacts demonstrated in Figs. 2 and 3 closely related to the coupled empirical formulas describing the non-linear variation of soil parameters. These soil parameters not only depended on the void ratio and effective stress, but also related to other factors such as soil fabric, degree of saturation, and chemical reactions. Therefore, further investigations were still needed to develop more comprehensive relationships to account for the variation of soil parameters during electro-osmotic consolidation.

4. A case study of electro-osmotic consolidation

4.1. Geological conditions of the field

Burnotte et al. (2004) reported a large field test located near Mont St-Hilaire in the St. Lawrence valley, about 40 km east of Montréal, Canada. The main purpose of this field test was to improve the strength of the soft clay in the foundation of an existing embankment and eliminate ongoing long-term settlement of the embankment. On the top of the treated area, there was a 2 m deep granular fill layer from the elevation of 40.5–38.5 m. Beneath the granular fill layer was a 3.5 m deep silty soil layer from the elevation of 38.5–35.0 m, a 1.5 m deep clay crust layer from the elevation of 35.0–33.5 m, and soft clay from the elevation of 33.5 m down. The soft clay submitted to electro-osmotic consolidation was normally consolidated and located at 9 m (elevation of 31.5 m) to 14 m (elevation of 26.5 m) below the ground surface. The basic properties of the treated soft clay were summarized in Table 2.

Table 2
Geotechnical properties of the treated soft clay from Burnotte et al. (2004).

Properties	Values
Water content, w (%)	50–70
Liquid limit, w_L (%)	56–66
Plastic limit, w_p (%)	24
Undrained shear strength, C_u (kPa)	28–35
Relative density, D_r	2.79
< 2 μm content (%)	70–80
Hydraulic conductivity, k_h ($\times 10^{-9}$ m/s)	1–2

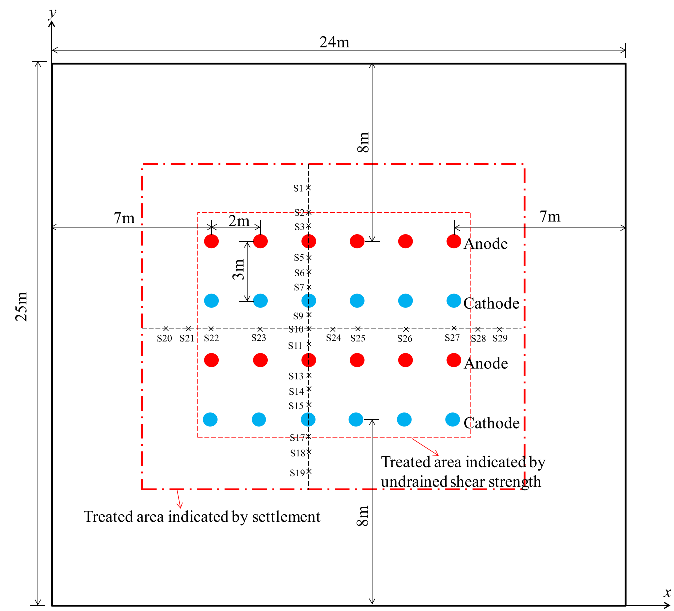

Fig. 4. Arrangement of electrodes and settlement marks.

4.2. Design of the field test

Twenty-four 14 m long pipes were installed vertically in the ground as electrodes, with an outside diameter of 0.17 m. The anode consisted of a 5 m long steel pipes positioned between elevations 31.5 m and 26.5 m, and a 9 m long PVC tubing positioned between elevations 40.5 m and 31.5 m. The cathodes were slotted steel pipes and installed from the ground surface down to 14 m (elevation of 26.5 m). These electrodes were arranged at 2 m intervals in rows with a space of 3 m between the anode and the cathode as shown in Fig. 4.

The electro-osmotic consolidation treatment lasted for 60 days including 12 days of current intermittence. The power system was first shut off for 3 days after 12 days of treatment, then for 7 days after day 25, and lastly for 2 days after day 44. During the 48 days of power-on periods, the applied voltage was not constant. According to Burnotte et al. (2004), the voltage gradient in the field was 0.33 V/cm in the first 22 power-on days, then reduced to 0.23 V/cm in the following 8 power-on days, and finally restored to 0.33 V/cm in the last 18 power-on days (Fig. 5).

The ground surface settlement was monitored by 25 settlement points once a week as illustrated in Fig. 4 (S1 to S29). The temperature, current, voltage between each pair of electrodes and drainage flow during the treatment were also monitored. After the field test, 22 Nilcon vane profiles were performed to characterize the increase in the undrained shear strength (C_u). In the following analysis, the surface settlements from field measurement and numerical simulations were compared to verify the effectiveness of the numerical model and investigate the impact of the non-linear variation of soil parameters.

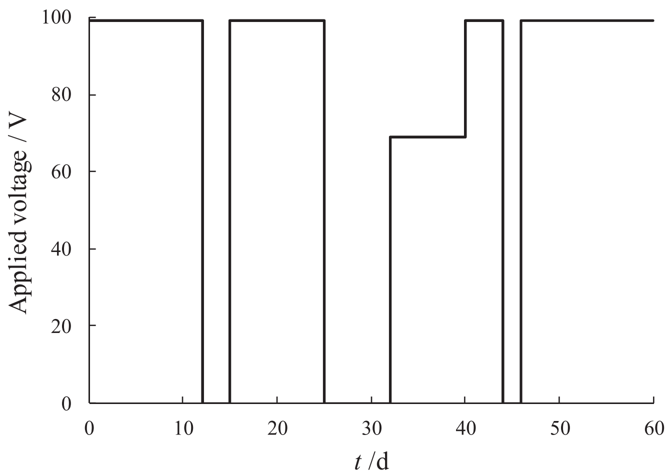

Fig. 5. Applied voltage in the field test.

4.3. Non-linear variation of soil parameters

As mentioned before, during electro-osmotic consolidation, soil parameters changed with the drainage and consolidation of the soil mass. In the field test, Burnotte et al. (2004) calculated the electro-osmosis conductivity from flow measurement at different treatment times as shown in Fig. 6. A non-linear relationship between electro-osmosis conductivity and treatment time was therefore obtained from the calculated values as the solid line shown in Fig. 6. The relationship was then incorporated into the numerical simulations. In addition, Burnotte et al. (2004) also conducted a compression test on the soft clay, and the obtained relationship between void ratio and effective stress was also coupled into the numerical simulations to describe the non-linear variation of the coefficient of compressibility. Therefore, the following numerical simulations mainly examined the impact of the non-linear variation of electro-osmosis conductivity and coefficient of compressibility.

4.4. Numerical simulation of the field test

According to the measured undrained shear strength after the treatment, the area affected by electro-osmotic consolidation extended laterally 0.5 m at the end of the electrode rows in the x direction, while in the y direction, the area extended 1 m behind the last row of anodes and 0.5 m behind the last row of cathodes (as shown by the dotted line in Fig. 4). The ground surface settlements indicated a relative larger

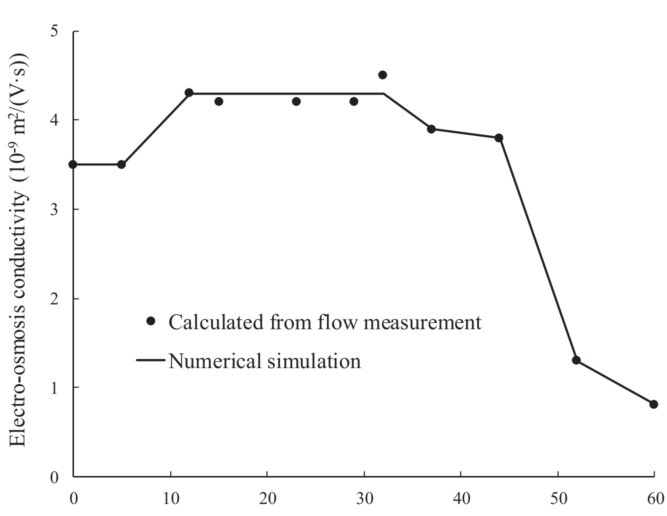

Fig. 6. Electro-osmosis conductivity for numerical simulation.

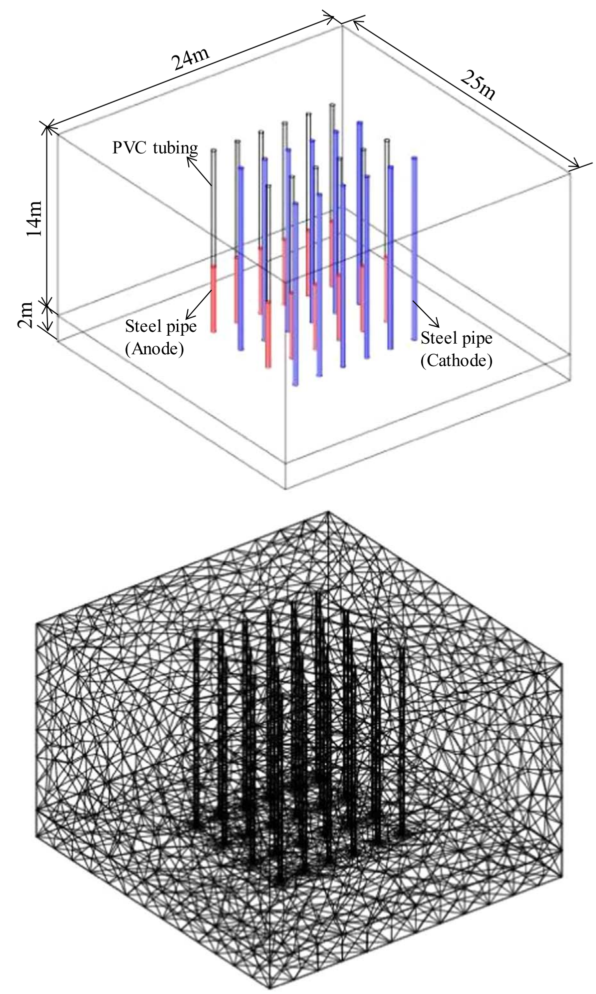

Fig. 7. The 3D numerical model and finite element mesh (Burnotte et al., 2004).

treated area, with an extension of about 6 m in the x direction and about 9 m in the y direction (as shown by the dot dash line in Fig. 4). In the z direction, according to Burnotte et al. (2004), the treated zone would extend 1 m below the position of the active electrodes. Therefore, a 24 m×25 m×16 m model was developed for numerical simulation in order to cover the area affected by electro-osmotic consolidation (as shown by the solid line in Fig. 4). Fig. 7 showed the 3D numerical model for this case study and the corresponding finite element mesh which contained 9359 nodes and 47,285 tetrahedral finite elements.

In the numerical simulations, pore water was allowed to flow out at the cathode and the top boundaries, and the other boundaries were set to be impermeable. The voltage in Fig. 5 was applied to the active part of the anode, i.e., the steel pipes from the elevation of 31.5–26.5 m. The peripheral boundary of the model was set to be fixed in horizontal direction and free in vertical direction, and the bottom boundary was set to be fixed in both directions.

Totally 4 numerical simulations were carried out: 1) In simulation 1 (N1), the soil parameters were set to be constant; 2) In simulation 2 (N2), the non-linear variation of electro-osmosis conductivity was coupled; 3) In simulation 3 (N3), the non-linear variation of coefficient of compressibility was coupled; 4) In simulation 4 (N4), both the non-linear variations of the electro-osmosis conductivity and coefficient of compressibility were coupled. The soil parameters adopted in the numerical simulations were listed in Table 3.

Table 3
Soil parameters adopted in the numerical simulations.

Properties	Values
Hydraulic conductivity, k_h (m/s)	1.2×10^{-9}
Initial electro-osmosis conductivity, k_{e0} (m^2/(V s))	3.5×10^{-9}
Initial Young's modulus, E_0 (kPa)	480
Electrical conductivity, σ_e (S/m)	0.02
Poisson's ratio, ν	0.35
Unit weight, γ (kN/m^3)	16.3

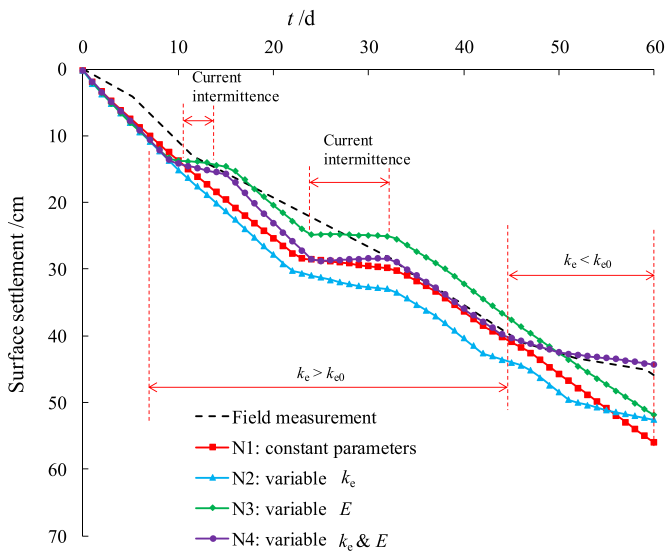

Fig. 8. Comparison of the surface settlement between field measurement and numerical simulations.

5. Results and discussion

Fig. 8 compared the surface settlement from field measurements (S6) and the calculation results from the four numerical simulations. Although slightly larger in the early period, the settlements from the numerical simulation considering both the non-linear variations of electro-osmosis conductivity and coefficient of compressibility (N4) coincided well with the field measurements, and the prediction of the settlement from N4 was more accurate than that from N1, N2 and N3, especially in the later period. According to the reported electro-osmosis conductivity shown Fig. 6, k_e increased from 3.5×10^{-9} m^2/(V s) to about 4.3×10^{-9} m^2/(V s) at around day 10, and kept constant till day 32, and then decreased to about 3.8×10^{-9} m^2/(V s) at about day 44, 1.3×10^{-9} m^2/(V s) at about day 52, and 8.1×10^{-10} m^2/(V s) at the end of the treatment. As a result, the settlements from the four numerical simulations were almost the same in the first 10 days, and afterwards, the settlements from N2 and N4 became larger than that from N1 and N3, respectively, due to the increase in k_e. After day 44, k_e decreased rapidly, therefore the development of settlement in N2 and N4 became slower than that in N1 and N3, respectively. The field measurement shown in Fig. 8 also illustrated a remarkable slower settlement development after day 44. Both the comparisons between N1 and N3 and that between N2 and N4 showed the effect of the non-linear variation of the coefficient of compressibility. As mentioned before, m_v decreased with the increase in effective stress during electro-osmotic consolidation treatment, which then led to a smaller settlement in N3 and N4 compared to that in N1 and N2, respectively.

The effect of current intermittence on the development of settlement was more significant when the non-linear variation of m_v was taken into account in the numerical simulation. The first current intermittence occurred from day 13 to day 15 and the development of the settlement in N3 and N4 slowed down during this period. The second current intermittence occurred from day 26 to day 32. During this period, all the four numerical simulations presented significant slower settlement development, and N3 and N4 showed an even smaller one than N1 and N2.

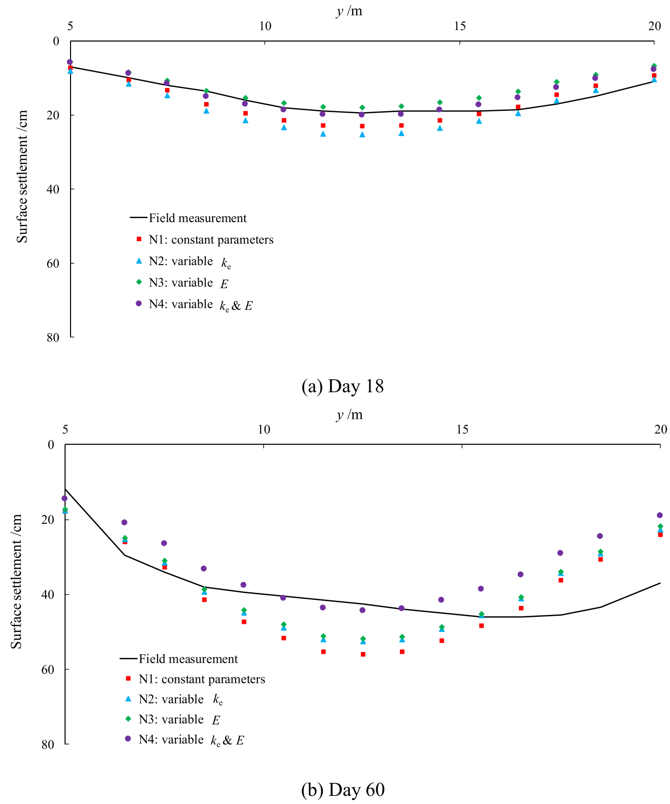

Fig. 9. Comparison of the surface settlement profile between field measurements and numerical simulations along y direction.

The ground surface settlement at different times was monitored by the 25 settlement points located along the x and y directions, respectively (Fig. 4). Figs. 9 and 10 compared the settlement profiles at 18 and 60 days of the treatment obtained from field measurements and numerical simulations. Both the field measurements and numerical simulations showed a bowl-shaped settlement profile along the x and y directions. The numerical simulation coupling both the non-linear variation of k_e and m_v demonstrated the best agreement with the field measurements among the four numerical simulations. However, compared to the numerical simulations, the field measurements showed a settlement profile steeper on the two sides and more subdued in the middle, and the settlement from the field measurements was actually larger than that from the numerical simulations on the two sides and slightly smaller in the middle. The deviation between field measurements and numerical simulations mainly resulted from the adoption of elastic constitutive model instead of elastoplastic constitutive model which was more realistic for soft soil. Future work will focus on the improvement of the numerical model for electro-osmotic consolidation by considering more realistic situation such as more sophisticated constitutive model and the numerical model for large strain behavior.

6. Conclusions

A 3D multi-field coupling numerical model for electro-osmotic consolidation was employed to analyze the effect of the non-linear variation of soil parameters during the consolidation process. The complex operating conditions, including boundary conditions and geometry, irregular electrode configuration, and current intermittence were simulated. A case study was performed to further verify the

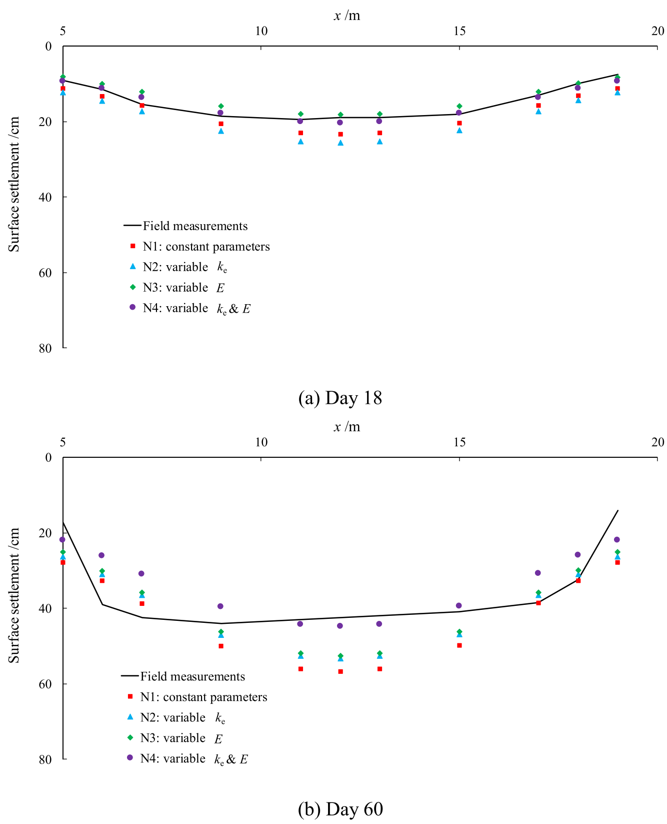

Fig. 10. Comparison of the surface settlement profile between field measurements and numerical simulations along x direction.

effectiveness of the numerical model. The following conclusions can be drawn based on the above studies.

The ignorance of stress-strain field led to a larger excess pore water pressure (absolute value) and degree of consolidation. The non-linear variation of soil parameters presented remarkable impact on electro-osmotic consolidation process. For the axisymmetric model studied, the non-linear variation of electro-osmosis conductivity and electrical conductivity caused a slightly smaller excess pore water pressure (absolute value), while the non-linear variation of hydraulic conductivity and coefficient of compressibility resulted in a larger one. The degree of consolidation was smaller with variable hydraulic conductivity and larger with variable coefficient of compressibility.

The predicted settlement from the numerical simulations coincided well with the field measurements when both the non-linear variation of electro-osmosis conductivity and coefficient of compressibility were considered, indicating that the numerical model was capable to analyze practical problems with complex operating conditions. The intermittence of current also showed remarkable impact on the electro-osmotic consolidation process, thus, the development of surface settlement was retarded when the applied current was interrupted. Moreover, the impact of current intermittence was more remarkable if the non-linear variation of the coefficient of compressibility was taken into account in the numerical simulation.

Acknowledgements

Financial support from the National Natural Science Foundation of China (Project No. 51579132, 51323014, 51609123), the Ministry of Education (Project No. THZ-02-2), and the China Postdoctoral Science Foundation (Grant No. 2015M581104) are gratefully acknowledged.

References

Archie, G.E., 1942. Electrical resistivity log as an aid in determining some reservoir characteristics. Trans. Am. Inst. Min. Eng. 146, 54–61.
Biot, M.A., 1941. General theory for three-dimensional consolidation. J. Appl. Phys. 12 (2), 155–164.
Bjerrum, L., Moum, J., Eide, O., 1967. Application of electroosmosis to a foundation problem in Norwegian quick clay. Géotechnique 17 (3), 214–235.
Burnotte, F., Lefebvre, G., Grondin, G., 2004. A case record of electro-osmotic consolidation of soft clay with improved soil-electrode contact. Can. Geotech. J. 41, 1038–1053.
Casagrande, L., 1983. Stabilization of soils by means of electroosmotic state-of-art. J. Boston Soc. Civ. Eng. ASCE 69 (3), 255–302.
Deng, A., Zhou, Y.D., 2015. Modeling electroosmosis and surcharge preloading consolidation. I: model formulation. J. Geotech. Geoenviron. Eng., (04015093-1).
Esrig, M.L., Gemeinhardt, J.P., 1967. Electrokinetic stabilization of an illitic clay. J. Soil Mech. Found. Div. 92 (SM3), 109–128.
Esrig, M.I., 1968. Pore pressures, consolidation and electro-kinetics. J. Soil Mech. Found. Eng. Div. ASCE 94 (SM4), 899–921.
Glendinning, S., Lamont-Black, J., Jones, C.J.F.P., 2007. Treatment of lagooned sewage sludge in situ using electrokinetic geosynthetics. J. Hazard. Mater. A139, 491–499.
Hu, L.M., Wu, H., 2014. Mathematical model of electro-osmotic consolidation for soft ground improvement. Géotechnique 64 (2), 155–164.
Hu, L.M., Wu, H., Wen, Q.B., 2013. Electro-osmotic consolidation: Laboratory tests and numerical simulation. In: Proceedings of the 18th International Conference on Soil Mechanics and Geotechnical Engineering. Paris, France.
Hu, L.M., Wu, W.L., Wu, H., 2010. Theoretical analysis and numerical simulation of electro-osmosis consolidation for soft clay. Rock. Soil Mech. 31 (12), 3977–3983, (in Chinese).
Hu, L.M., Wu, W.L., Wu, H., 2012. Numerical model of electro-osmotic consolidation in clay. Géotechnique 62 (6), 537–541.
Jeyakanthan, V., Gnanendran, C.T., Lo, S.C.R., 2011. Laboratory assessment of electro-osmotic stabilization of soft clay. Can. Geotech. J. 48 (12), 1788–1802.
Jeyakanthan, V., Gnanendran, C.T., 2013. Elastoplastic numerical approach for predicting the electro-osmotic consolidation behaviour of soft clays. Can. Geotech. J. 50 (12), 1219–1235.
Lewis, R.W., Humpheson, C., 1973. Numerical analysis of electro-osmotic flow in soils. J. Soil Mech. Found. Div. ASCE 99 (SM8), 603–616.
Li, Y., Gong, X.N., Lu, M.M., Guo, B., 2010. Coupling consolidation theory under combined action of load and electro-osmosis. Chin. J. Geotech. Eng. 32 (1), 77–81.
Lo, K.Y., Ho, K.S., Inculet, I.I., 1991. Field test of electroosmotic strengthening of soft sensitive clay. Can. Geotech. J. 20 (1), 74–83.
Lockhart, N.C., 1983. Electroosmotic dewatering of clays, III. Influence of clay type, exchangeable cations, and electrode materials. Colloids Surf. 6 (3), 253–269.
Micic, S., Shang, J.Q., Lo, K.Y., Lee, Y.N., Lee, S.W., 2001. Electro-kinetic strengthening of a marine sediment using intermittent current. Can. Geotech. J. 38 (22), 287–302.
Mitchell, J.K., Soga, K., 2005. Fundamentals of Soil Behavior 3rd ed.. John Wiley & Sons, Inc, USA.
Rittirong, A., Shang, J.Q., 2008. Numerical analysis for electro-osmotic consolidation in two-dimensional electric field. In: Proceedings of the 18th ISOPE. Vancouver, Canada, pp. 566–572.
Shang, J.Q., 1998. Electroosmotic enhanced preloading consolidation via vertical drains. Can. Geotech. J. 35 (3), 491–499.
Su, J.Q., Wang, Z., 2003. Theory of two-dimensional electro-osmotic consolidation of soils. Geotechnique 53 (8), 759–763.
Wan, T.Y., Mitchell, J.K., 1976. Electro-osmotic consolidation of soils. J. Geotech. Eng. Div. ASCE 102 (GT5), 473–491.
Wang, L.J., Liu, S.H., Wang, J.B., Zhu, H., 2012. Numerical analysis of electroosmotic consolidation based on coupled electrical field-seepage field-stress field. Rock. Soil Mech. 33 (6), 1904–1911.
Wu, H., Hu, L.M., 2013a. Numerical simulation of electro-osmosis consolidation considering variation of electrical conductivity. Chin. J. Geotech. Eng. 35 (4), 734–738, (in Chinese).
Wu, H., Hu, L.M., 2013b. Analytical solution for axisymmetric electro-osmotic consolidation. Géotechnique 63 (12), 1074–1079.
Wu, H., Hu, L.M., 2014. Microfabric change of electro-osmotic stabilized bentonite. Appl. Clay Sci. 101 (11), 503–509.
Wu, H., Hu, L.M., Zhang, G.P., 2016. Effects of electro-osmosis on the physical and chemical properties of bentonite. J. Mater. Civ. Eng., 06016010–06016011.
Wu, H., Hu, L.M., Zhang, L., Wen, Q.B., 2015a. Transport and exchange behavior of ions in bentonite during electro-osmotic consolidation. Clays Clay Miner. 63 (5), 395–403.
Wu, H., Hu, L.M., Wen, Q.B., 2015b. Electro-osmotic enhancement of bentonite with reactive and inert electrodes. Appl. Clay Sci. 111 (7), 76–82.
Wu, H., Qi, W.Q., Hu, L.M., Wen, Q.B., 2017. Electro-osmotic consolidation of soil with variable compressibility, hydraulic conductivity and electro-osmosis conductivity. Comput. Geotech. 85, 126–138.
Xu, W., Liu, S.H., Wang, L.J., Wang, J.B., 2011. Analytical theory of soft ground consolidation under vacuum preloading combined with electro-osmosis. J. Hohai Univ. (Nat. Sci.) 39 (2), 169–175, (in Chinese).
Zhou, Y.D., Deng, A., Wang, C., 2013. Finite-difference model for one-dimensional electro-osmotic consolidation. Comput. Geotech. 54, 152–165.
Yuan, L., Hicks, M.A., 2015. Numerical analysis of electro-osmosis consolidation: a case study. Géotech. Lett. 5, 147–152.